GEOPHYSICAL RESEARCH LETTERS, VOL. 23, NO. 6, PAGES 649-652, MARCH 15, 1996

Sprites as luminous columns of ionization produced by quasi-electrostatic thundercloud fields

V.P. Pasko, U.S. Inan, and T.F. Bell
STAR Laboratory, Stanford University, Stanford, California

Abstract. Quasi-electrostatic (QE) fields which exist above thunderclouds after lightning discharges can lead to the formation of columnar channels of breakdown ionization and carrot-like vertical luminous structures with typical transverse dimension ~5-10 km spaning an altitude range from ~80 km to well below ~50 km. The carrot-like forms closely resemble those observed in sprites. Results indicate that the appearance of optical emissions can be significantly delayed in time (~1-20 ms) with respect to the causative lightning discharge.

Introduction

Sprites are luminous glows occurring at altitudes typically ranging from ~50 to 90 km [e.g., *Sentman et al.*, 1995; *Rairden and Mende*, 1995]. In video they exhibit a red color which gradually changes to blue below ~50 km. The red color is primarily due to excitation of the 1st positive band of N_2 ($N_2 1P$) [*Mende et al.*, 1995; *Hampton et al.*, 1996]. Sprites are associated with energetic positive cloud-to-ground lightning discharges (CGD) [e.g., *Boccippio et al.*, 1995], endure for several ms, and are typically delayed in time ranging from ~3 ms [*Winckler et al.*, 1995] to several tens of ms [*Fukunishi et al.*, 1995] with respect to the onset of the causative CGD. Sprites may occur singly or in clusters of two or more. The lateral extent of 'unit' sprites is typically 5-10 km [*Sentman et al.*, 1995], however, they can occupy much larger volumes (e.g., 50x50 km) [*Winckler et al.*, 1995]. Mechanisms for sprites include heating of the ionospheric electrons by the electromagnetic pulse (EMP) from lightning [*Inan et al.*, 1996 and references therein] or by large QE fields [*Wilson*, 1925; *Pasko et al.*, 1995; *Winckler et al.*, 1995; *Boccippio et al.*, 1995], as well as runaway electron (REL) processes [*Bell et al.*, 1995; *Winckler et al.*, 1995; *Taranenko and Roussel-Dupre*, 1995].

Large electric field (E) transients capable of causing breakdown ionization at mesospheric altitudes can be produced by induced spatially distributed space charge which exists in the region between the thundercloud tops and the lower ionosphere following the removal of a thundercloud charge (Q) by a CGD [*Pasko et al.*, 1995]. Depending on the history of charge accumulation and removal and distribution of ambient atmospheric conductivity (σ) the breakdown region may have the shape of ionization column(s) which electrically connect the induced charges and the highly conducting lower ionosphere. Formation of these ionization columns may be closely associated with streamer type processes characterized as filamentary plasmas, the dynamics of which are controlled by highly localized nonlinear space charge waves [e.g., *Uman*, 1984, p. 202; *Vitello et al.*, 1994]. An ionization channel may develop from a seed enhancement of local conductivity of any origin (see next sections) and physically its propagation is controlled by the relaxation of the electric filed inside its conducting body and enhancement of the field in the vicinity of its tip, much like that near the curved boundaries of conducting bodies in an E field. The time history of charge removal from the thundercloud can lead to the creation of a variety of shapes and dynamics of sprites.

In this paper we evaluate ionization changes and optical emission intensities (I) as a function of the time history of charge removal by a CGD. Results are compared with video, photometric and spectroscopic observations.

Paper number 96GL00473
0094-8534/96/96GL-00473$03.00

Model

Cylindrical coordinates (r, ϕ, z) are used with the z axis representing altitude. Electric field E, charge density ρ, electron density N_e and emission intensity I are calculated as described in [*Pasko et al.*, 1995] with the same ambient conditions (N_e and ion σ profiles). In contrast with the two-fluid approach of [*Vitello et al.*, 1994] the model of [*Pasko et al.*, 1995] is based on the continuity equation for ρ and may not accurately predict the small scale details of N_e near the steep boundaries associated with the front of ionization channels. Calculations indicate that downward propagating ionization channels tend to focus to very sharp edges which often lead to numerical instability at low altitudes (~50 km). For modeling of the downward propagation we somewhat arbitrarily introduce in our model an 'effective' recombination constant α=1 cm^3/s at 50 km which varies exponentially in altitude with a scale height of 6 km, accounting for the increasing electron losses at low altitudes, and also serves as a smoothing factor preventing unphysically large oscillations in N_e. For modeling of upward propagating channels which can be launched from seeds of plasma at low altitudes (see next section) we assume that the dielectric relaxation time (ε_o/σ) behind the front of the channel remains constant in accordance with the results of extensive streamer simulations [e.g., *Vitello et al.*, 1994]. The thundercloud charges $+Q$, $-Q$ ($+Q$ placed at 10 km) form a vertical dipole which develops over several tens of seconds. The $+Q$ charge is then rapidly discharged to the ground. The response of the system at mesospheric altitudes depends on the altitude and magnitude of $+Q$ and does not depend on the initial charge configuration inside the cloud (i.e., magnitude and altitude of $-Q$) [*Pasko et al.*, 1995].

The optical excitation rates for selected bands are calculated using integral cross sections which do not provide information about the particular wavelength of emitted photons [*Taranenko et al.*, 1993]. Typical video cameras have well defined red, green, and blue filters [e.g., *Wescott et al.*, 1995, Figure 5] which extract only a very narrow part of the spectrum in the visible range of wavelengths. To determine the number of photons corresponding to $N_2 1P$ which produces, for example, the red video response, one needs to integrate the normalized distribution of emissions in different wavelengths inside the band and the corresponding red filter. This consideration is important since only a small fraction of the energy of $N_2 1P$ is in the visible region. On

the basis of spectral observations of $N_2 1P$ associated with sprites [*Mende et al.*, 1995; *Hampton et al.*, 1996] the distribution of intensities of the different wavelengths can be assumed to be the same as in the aurora [*Vallance Jones*, 1974, pp.129-132,139]. Calculations show that $N_2 1P$ and 2nd positive ($N_2 2P$) bands produce the largest red and blue video response, respectively. Only 1 % of the total number of emitted photons corresponding to $N_2 1P$ appear in the pass band of the red filter of the video camera. The corresponding scaling factor for the blue $N_2 2P$ is 2.9 %. The ambient nighttime I of $N_2 1P$ is $\sim 10^4$ R [*Chamberlain*, 1978, pp. 214-218], so that the total integral I (as calculated in our model) should be at least 10^6 R to be observable in video. For this reason, we show I in Figures 2 and 3 on a scale starting from 10^6 R.

The top panels of Figure 1 show five different models of charge removal used in this work. The time t=0 corresponds to the beginning of charge removal.

Results

Electron Number Density. Results of calculations of N_e as a function of t corresponding to case e in Figure 1 are shown in Figure 2a. At t=2 ms, a region of significant ionization at 70-80 km altitudes and with characteristic radius >10 km is produced by the fast (1 ms) removal of the first 200 C, similar to the cases studied earlier [*Pasko et al.*, 1995]. Although E is enhanced just outside of this localized region of enhanced conductivity, this increase is compensated by the relatively high ambient conductivity at these altitudes, inhibiting the formation of an ionization channel. If removal of charge in this case were limited to 200 C no ionization channel would be formed. In most cases, however, fast impulsive removal of charge is followed by a period of continuing current which usually lasts tens of ms and can account for a significant fraction of the total charge lowered by a CGD [*Uman*, 1987, pp. 196, 200]. Such low rates of charge removal can in some cases further increase the curvature of the highly conducting region leading to the formation of channels of breakdown ionization propagating downward as shown in Figure 2a. Focusing (Figure 2a, t =10 ms) and subsequent expansion (Figure 2a, t =20 ms) of ionization toward lower altitudes is caused by the fact that the additional slow charge removal enhances E and widens the region of breakdown ionization. This behavior occurs at altitudes (<60km) where the ambient conductivity is low enough that it does not prevent enhancement of E near the tip of the channel in contrast with high altitudes ($\sim$ 70 km).

Electric Field. The spatial distribution of E at different time intervals are shown in Figure 2b normalized to E at t = 15 ms. The normalization is performed to demonstrate the enhancement of E in regions near the tip of the ionization channel. The characteristic breakdown field E_k [*Papadopoulos et al.*, 1993] is also shown in the top panel of Figure 2b. E is always approximately equal to E_k at the tip of the channel. Physically, when E exceeds E_k, ionization increases lead to enhanced local conductivity which in turn leads to the rapid relaxation of E. As a result, E tends to remain near E_k.

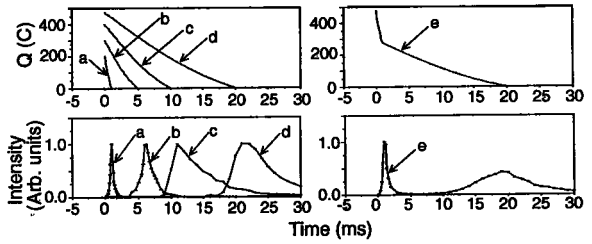

Figure 1. *Top panels.* Five models of thundercloud charge removal used in calculations: (a) removal of 200 C of Q in 1 ms; (b) 300 C in 5 ms; (c) 400 C in 10 ms; (d) 475 C in 20 ms; (e) fast initial removal of 200 C in 1 ms and then slow removal of 275 C in 19 ms. *Bottom panels.* Corresponding spatially integrated I as a function of t.

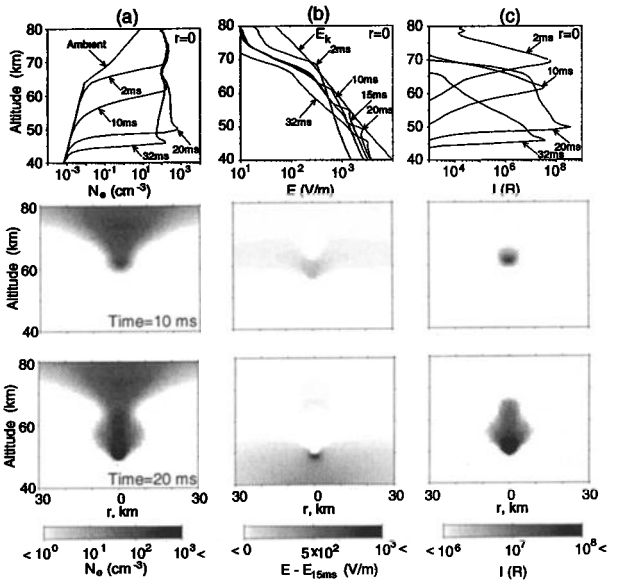

Figure 2. A crossectional view of the distribution of N_e (a), absolute values of E (b), and I of $N_2 1P$ (c) at selected instants of time. Top panels show altitude scans at $r = 0$.

Optical emissions. The emission intensity corresponding to $N_2 1P$ is shown in Figure 2c, and is significant only in regions where E is above the threshold of excitation of N_2. Significantly reduced E inside the ionized regions (Figure 2a) results in insignificant optical output. The optical emission region is rather wide ($\sim$20 km) at t=2 ms at altitudes $\sim$70 km but subsequently becomes narrower ($\sim$5 km) at altitudes $\sim$60 km at t=10 ms, and expands downward at later times. Downward propagation slows down below $\sim$50 km altitudes due to the exponential increase in electron loss at these altitudes. The average speed of downward propagation of the sprite is $\sim 10^3$ km/s.

The optical emissions usually endure for times less than or comparable to the duration of one video frame (1/30 sec). For comparison with video observations it is useful to average over $\sim$30 ms. Figure 3 shows distributions of the $N_2 1P$ intensity averaged over 32 ms for cases b,c,d, and e and over 4 ms for the case a. In case b we place a 'ball' of highly conducting plasma with radius $\sim$5 km and $N_e \sim 10^4 \mathrm{cm}^{-3}$ at altitude 45 km. The ionization channel is initiated in this case at altitude $\sim$50 km due to the enhanced conductivity and associated E and propagates upward showing slight expansion toward higher altitudes. The estimated propagation speed was very high ($\sim 10^4$ km/s) and was mostly defined by almost simultaneous enhancement of E above E_k in a region between the charge induced in the tip of the streamer and the upper boundary of the simulation at 80 km. For case b E reaches E_k only at the very end of charge removal at $t \sim$10 ms, so that we see self driven development of an ionization channel propagating downward which tends to focus toward lower altitudes. For case d, the total amount of removed

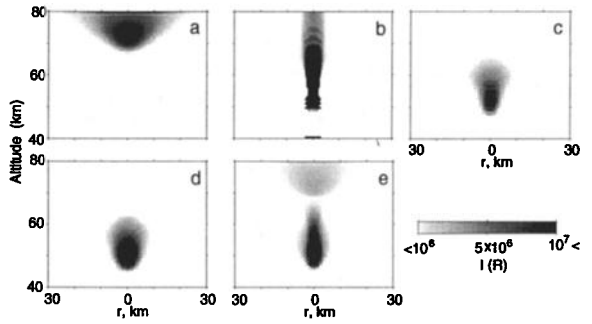

Figure 3. The distribution of time averaged I (Rayleighs) of $N_2 1P$ is shown on linear scale and for models of charge removal as illustrated in Figure 1.

charge (475 C) is greater than for case c (400 C) so that E exceeds E_k over a larger region and the corresponding structure of the optical emissions appears to be wider and does not show significant focusing toward lower altitudes. Case e shows structure consisting of two parts separated by a gap at altitudes $\sim$ 67 km. This feature is consistent with typical structure of sprites as a high altitude 'plume' and adjacent lower altitude 'dendritic' (forked) forms [e.g., *Winckler et al.*,1995].

Discussion

Comparison With Video Observations. Figure 4b shows the expected red and blue video response, calculated through the procedure described in previous sections, at t=20 ms for case e. The blue color becomes increasingly important at lower altitudes, being only a factor of 2 below the red at $\sim$50 km. Below $\sim$ 40 km, blue becomes the dominant color, in agreement with observations of sprites [*Sentman et al.*, 1995]. The range of I (10^2-10^3 kR) shown in Figure 4b is consistent with video observations [*Sentman et al.*, 1995].

The variety of sprite shapes shown in Figure 3 are within the range of the measured transverse and horizontal sizes of sprites. However, the five cases shown in Figure 3 do not represent all possible shapes which are observed or which can occur under different conditions. Model calculations (not shown) indicate that the transverse size of sprites can be very large (e.g., $\sim$ 50x50 km as reported in [*Winckler et al.*, 1995]) depending primarily on the total amount of charge removed from the thundercloud (i.e., effective volume of space in which the post discharge E exceeds E_k), the dynamics of charge removal, and the ambient conductivity profile. Localized conductivity enhancements (e.g., case b) which occur due to external sources (i.e., electron precipitation from the magnetosphere, meteors, runaway electrons, perturbations

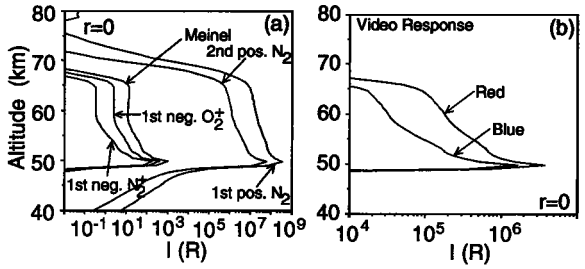

Figure 4. (a) Altitude scans at (r=0) of I corresponding to different optical bands. (b) Expected red and blue video response corresponding to optical emissions shown in (a).

left from a previous sprite, etc.) may significantly enhance E and control the transverse scale of ionization channels and explain how one CGD can create clusters of sprites. Under certain conditions such preexisting enhancements of conductivity may stimulate both upward going (toward ionosphere) and downgoing channels of ionization. Furthermore, the removal of large amounts of positive charge from the lower part of the thundercloud as suggested by [*Winckler et al.*, 1995; *Boccippio et al.*, 1995; *E. Williams*, private communication] may produce simultaneous upward going (from the cloud tops) and down going (from the ionosphere) streamers of ionization. Streamer processes may also account for the dynamics of blue jets [*Wescott et al.*, 1995], which might be initiated during the thundercloud charge accumulation phase prior to lightning discharges.

Results of [*Fukunishi et al.*, 1995] suggest the duration of sprites is $\sim$2 ms measured between 3 dB intensity points. On the other hand results of [*Rairden and Mende*, 1995] suggest the duration may be as large as $\sim$40 ms. A conduction current always exist in the body of the ionization channel as it propagates due to the finite $E \leq E_k$ (e.g., Figure 2b, t =2,10,15,20ms), and decays as soon as the channel stops (e.g., Figure 2b, t=32 ms). The observed persistence of luminosity of sprites for several tens of ms [*Rairden and Mende*, 1995] is a strong indication of the persistence of associated E and current flow in the body of the sprite. The effect of sprites is to transfer to the conducting ionosphere the distributed charges between the tops of thunderclouds and the lower ionosphere induced prior to CGD [*Pasko et al.*, 1995].

The conservation of current within the streamer body as it propagates in the atmosphere requires focusing of the channel propagating downward and expansion of the channel propagating upward. Ambipolar diffusion of electrons may stop the focusing process as soon as the sprite has a cross section $\leq 10^3 m^2$ at $\sim$50 km and may lead to the splitting of sprite in many small scale filaments. The splitting process can not be properly modeled with our azimuthally symmetric model, however the model reproduces reasonably well the dynamics of the decay of luminosity which first starts at high altitudes (Figure 2c, top panel) in agreement with observations [*Rairden and Mende*, 1995].

Comparison With Photometric Observations. Figure 1 (bottom panels) shows results of spatially integrated I as a function of t for cases a,b,c,d, and e shown in Figure 1 (top panels). The onset of the optical emission does not necessarily coincide with the onset of the causative CGD and can in fact be significantly delayed in time (up to $\sim$20 ms for the case d). This result is in agreement with photometric measurements by *Winckler et al.* [1995] who reported delays $\sim$3 ms, and by *Fukunishi et al.* [1995] showing delays ranging from several ms and up to several tens of ms. Physically, this effect is explained in terms of the threshold dependence of the optical emissions and ionization processes on E. Optical emissions appear nearly instantaneously in time when the corresponding threshold is reached. Results in Figure 1 for the cases a and e show short pulses with duration $\sim$3 ms with respect to the onset of causative CGD which are created by the fast removal of 200 C of charge in 1 ms. These few ms short pulses should not be confused with the ionospheric flashes produced by EMP-induced heating and observed within few hundred microseconds of the causative CGD [*Fukunishi et al.*, 1995; *Inan et al.*, 1996].

Comparison With Spectroscopic Observations. The altitude distribution of emission intensities corresponding to five different optical bands are shown in Figure 4a for case e and at t=20 ms. The emission levels in these bands depend on the value of E (i.e., level of electron heating) and N_e (ambient and produced due to ionization) and might be different for different altitudes and regimes of charge removal.

However, our calculations show that under QE heating conditions the Meinel band of N_2^+ and 1st negative band of O_2^+ only occasionally reach levels above those of the ambient nighttime airglow ($\sim 10^4$ R and $\sim 10^2$ R, respectively [*Chamberlain*, 1978, pp. 214-218]). $N_2 1P$ and $N_2 2P$ and the 1st negative band of N_2^+ have ambient levels of $\sim 10^4$ R, ~ 5 R, and ~ 5 R, respectively [*Chamberlain*, 1978, pp. 214-218], and under different QE heating conditions are excited at levels well above the ambient levels. Recent spectral measurements of sprites confirmed the existence of $N_2 1P$ [*Mende et al.*, 1995; *Hampton et al.*, 1996]. Most of the energy of $N_2 2P$ is concentrated in the wavelengths region of ~300-400 nm [*Vallance Jones*, 1974, Table 4.11, p. 131] which is below the spectral range resolved in *Mende et al.* [1995] (450-800 nm) and *Hampton et al.* [1996] (540-840 nm) measurements consistent with the fact that this band was not detected.

Summary

A QE model of lower ionospheric heating and ionization indicates that most of the observed features of sprites can be explained in terms of the formation and self-driven propagation of channels of breakdown ionization. Optical emissions of the dominant $N_2 1P$ and $N_2 2P$ form carrot-like vertical structures with typical transverse dimension ~5-10 km which can span altitude range from ~80 km to well below ~50 km. The appearance of optical emissions associated with sprites can be delayed in time (~1-20 ms) with respect to the causative CGD. Model results are found to be in good agreement with recent video, photometric and spectral measurements of sprites.

Acknowledgments. This work was sponsored by NASA grant NAGW-2871-2 to Stanford University.

References

Bell, T. F., V. P. Pasko, and U. S. Inan, Runaway electrons as a source of Red Sprites in the mesosphere, *Geophys. Res. Lett., 22*, 2127, 1995.

Boccippio, D.J., E. R. Williams, S. J. Heckman, W. A. Lyons, I. T. Baker, and R. Boldi, Sprites, ELF transients, and positive ground strokes,*Science,269,* 1088, 1995.

Chamberlain, J. W., *Theory of planetary atmospheres*, Academic Press, New York, 1978.

Fukunishi, H., Y. Takahashi, M. Kubota, K. Sakanoi, U. S. Inan, and W. A. Lyons, Lower ionospheric flashes induced by lightning discharges, *EOS, 76,* F114, A41D-7, 1995.

Hampton, D. L., M. J. Heavner, E. M. Wescott, and D. D. Sentman, Optical spectra of sprites, *Geophys. Res. Lett., 23*, 89, 1996.

Inan, U. S., W. A. Sampson, and Y. N. Taranenko, Space time structure of lower ionospheric optical flashes and ionization changes produced by lightning EMP, *Geophys. Res. Lett., 23,* 133, 1996.

Mende, S. B., R. L. Rairden, and G. R. Swenson, Sprite spectra: N_2 1 PG band identification, *Geophys. Res. Lett., 22*, 3468, 1995.

Papadopoulos, K., G. Milikh, A. Gurevich, A. Drobot, and R. Shanny, Ionization rates for atmospheric and ionospheric breakdown, *J. Geophys. Res., 98*, 17593, 1993.

Pasko, V. P., U. S. Inan, Y. N. Taranenko, and T. F. Bell, Heating, ionization and upward discharges in the mesosphere due to intense quasi-electrostatic thundercloud fields, *Geophys. Res. Lett., 22,* 365, 1995.

Rairden, R. L., and S. B. Mende, Time resolved sprite imagery, *Geophys. Res. Lett., 22,*3465, 1995.

Sentman, D. D., E. M. Wescott, D. L. Osborne, D. L. Hampton, M. J. Heavner, Preliminary results from the Sprites94 campaign: Red Sprites, *Geophys. Res. Lett., 22*, 1205, 1995.

Taranenko, Y. N., U. S. Inan and T. F. Bell, The interaction with the lower ionosphere of electromagnetic pulses form lightning: excitation of optical emissions, *Geophys. Res. Lett., 20*, 2675, 1993.

Taranenko, Y. N., and R. A. Roussel-Dupre, Upward discharges and gamma-ray flashes: Manifestation of runaway air breakdown, *1995 Annual CEDAR Meeting*, June 25-30, Boulder, Colorado.

Vallance Jones, A., *Aurora*, D. Reidel publishing Co., Dordrecht, 1974.

Vitello, P. A., B. M. Penetrante, and J. N. Bardsley, Simulation of negative-streamer dynamics in nitrogen, *Phys. Rev. E, 49,* 5574, 1994.

Wescott, E. M., D. Sentman, D. Osborne, D. Hampton, and M. Heavner, Preliminary results from the Sprites94 aircraft campaign: 2. Blue jets, *Geophys. Res. Lett., 22,* 1209, 1995.

Wilson, C. T. R., The electric field of a thundercloud and some of its effects, *Proc. Phys. Soc. London, 37*, 32D, 1925.

Winckler, J. R., W. A. Lyons, T. Nelson, and R. J. Nemzek, New high-resolution ground-based studies of cloud-ionosphere discharges over thunderstorms (CI or Sprites), *J. Geophys. Res.*, in press, 1995.

Uman, M.A., *The lightning discharge*, Academic Press, Orlando, 1987.

Uman, M. A., *Lightning*, Dover Publications, 1984.

V. P. Pasko, U. S. Inan, and T. F. Bell, STAR Laboratory, Stanford University, Stanford, CA 94305.

(received October 16, 1995;
revised January 10, 1996;
accepted January 23, 1996.)